Biochimica et Biophysica Acta, 1099 (1992) 102–110

BBABIO 43556

Influence of the size and protonation state of acidic residue 85 on the absorption spectrum and photoreaction of the bacteriorhodopsin chromophore

Janos K. Lanyi [a], Jörg Tittor [b], György Váró [a,1], Günther Krippahl [b] and Dieter Oesterhelt [b]

[a] *Department of Physiology and Biophysics, University of California, Irvine, CA (U.S.A.) and the* [b] *Max-Planck-Institut für Biochemie, Martinsried (Germany)*

(Received 24 July 1991)

Key words: Bacteriorhodopsin; Bacteriorhodopsin structure; Chromophore; (*Halobacterium sp.* GRB strain 384)

The consequences of replacing Asp-85 with glutamate in bacteriorhodopsin, as expressed in *Halobacterium* sp. GRB, were investigated. Similarly to the in vitro mutated and in *Escherichia coli* expressed protein, the chromophore was found to exist as a mixture of blue (absorption maximum 615 nm) and red (532 nm) forms, depending on the pH. However, we found two widely separated pK_a values (about 5.4 and 10.4 without added salt), arguing for two blue and two red forms in separate equilibria. Both blue and red forms of the protein are in the two-dimensional crystalline state. A single pK_a, such as in the *E. coli* expressed protein, was observed only after solubilization with detergent. The photocycle of the blue forms was determined at pH 4.0 with 610 nm photoexcitation, and that of the red forms at pH 10.5 and with 520 nm photoexcitation, in the time-range of 100 ns to 1 s. The blue forms produced no M, but a K- and an L-like intermediate, whose spectra and kinetics resembled those of blue wild-type bacteriorhodopsin below pH 3. The red forms produced a K-like intermediate, as well as M and N. Only the red forms transported protons. Specific perturbation of the neighborhood of the Schiff base by the replacement of Asp-85 with glutamate was suggested by (1) the shift and splitting of the pK_a for what is presumably the protonation of residue 85, (2) a 36 nm blue-shift in the absorption of the all-*trans* red chromophore and a 25 nm red-shift of the 13-*cis* N chromophore, as compared to wild-type bacteriorhodopsin and its N intermediate, and (3) significant acceleration of the deprotonation of the Schiff base at pH 7, but not of its reprotonation and the following steps in the photocycle.

Introduction

A great deal of evidence shows that proton transport in bacteriorhodopsin includes at least the following events: (1) light-induced isomerization of the retinal around the 13–14 carbon bond [2,29], (2) transfer of the Schiff base proton to Asp-85 and release of this or another proton from a nearby residue to the external side [3,4,33], (3) proton transfer from Asp-96 to the Schiff base [4,13,27,33], (4) reprotonation of Asp-96 from the cytoplasmic side and reisomerization of the retinal [15,27,36], and (5) return to the original state of bacteriorhodopsin. These events correspond, respectively, to the spectroscopically detectable transitions known as (1) BR $-h\nu \rightarrow$ J $\rightarrow$ K $\rightarrow$ KL $\rightarrow$ L, (2) L $\rightarrow$ M, (3) M $\rightarrow$ N, (4) N $\rightarrow$ O and N $\rightarrow$ BR, and (5) O $\rightarrow$ BR (reviewed in Ref. 35; for a recent report on the photocycle kinetics, cf. Ref. 42). In addition, the occurence of structural changes in the protein during proton transport was shown [17].

Studies of bacteriorhodopsins in which critical acidic residues, such as Asp-85 and Asp-96, were replaced with isomorphic but non-protonable or heteromorphic amino acids have contributed much to above scheme. We concentrate here on the Asp85 mutants. The chromophore spectrum in the Asp85 $\rightarrow$ Glu protein became greatly pH dependent in the physiological pH range: at pH below 6 a blue form, absorbing near 610 nm, predominated, while at higher pH a red form, absorb-

[1] Permanent address: Biological Research Center of the Hungarian Academy of Sciences, Szeged, Hungary.

Correspondence: D. Oesterhelt, Max-Planck-Institut für Biochemie, D-8033 Martinsried, Germany.

ing near 540 nm, was seen [4,28,32,36]. The equilibrium between these forms was affected by the nature of detergent also, when present (compare data in Refs. 24, 32 and 36). The red-blue transition resembled the purple-blue transition long known in wild-type bacteriorhodopsin [10,11,25,38], except that under similar conditions the latter occurred at about pH 3. This similarity, and the pH-independent blue color of the protein obtained when Asp-85 was replaced with a non-protonable residue [28,33,36], strongly suggested that the color change to blue was a consequence of the protonation of Asp-85. If this is so, the negative charge of the ionized Asp-85 is an important part of the counterion to the Schiff base. From a *C=O* stretch frequency of 1765 cm^{-1} in the *M* state an unusually low pK_a (2.5–3) for a carboxyl group involved in proton transport was expected [40], and could be assigned to Asp-85 [3]. The apparent stabilization of the ionized Asp-85 may be a consequence of interaction with the nearby positively charged Arg-82 residue. It seemed reasonable to suppose that Glu-85 was not in a position to interact as effectively with Arg-82, and the pK_a of this residue was thereby raised [28,36]. Consistent with this idea was the observation that replacement of Arg-82 with a neutral residue also raised the pK_a for the color change [34].

Some of the above results with Asp85 → Glu substitution were obtained with cloned and in vitro mutated bacteriorhodopsin expressed in *Escherichia coli* [24,28,36], others with in vivo mutated bacteriorhodopsin in *Halobacterium sp.* GRB selected for lack of phototrophic growth [4,32]. In this study we made use of the latter kind of samples where the protein is located, as wild-type bacteriorhodopsin, in two dimensional crystalline arrays (purple membranes) rather than in detergent micelles or reconstituted liposomes. The chromophore spectra indicated that this makes an important difference in the state of the Asp85 → Glu protein. We have also dissected the spectroscopic changes after flash excitation in these samples, and described the photocycles of the red and blue forms. Although the red form, whose absorption maximum is blue-shifted, produced a wild-type like M intermediate we found that one of the two other intermediates detected (the N species) had a red-shifted maximum relative to its wild-type equivalent. Thus, replacement of Asp-85 with glutamate appeared to shift the absorption band of the all-*trans* chromophore to lower wavelengths but that of the 13-*cis* chromophore to higher wavelengths.

Materials and Methods

Halobacterium sp. GRB strain 384 (Asp85 → Glu) was obtained earlier by mutagenesis of the wild-type GRB strain [42]. The cells were grown with low aeration and intense illumination in order to produce large amounts of the protein. The latter was isolated as previously described [26]. Solubilization, when required, was with 0.5% Triton X-100 at pH 7, by incubating 24 h at room temperature [8] after which time the samples did not sediment and exhibited the blue-shift characteristic of monomeric bacteriorhodopsin. For some measurements at lower pH the protein was encased in acrylamide gels [25] in order to prevent aggregation; other measurements were in suspensions. Cell envelope vesicles were prepared also as before [19].

For X-ray diffraction the samples were collected in 1 mm diameter capillaries by centrifugation, and exposed for 68 h to a 'fine focus' 0.1 × 1 mm beam from a Cu anode (40 kV, 30 mA). The powder-type diffraction pattern was recorded on film placed 10 cm from the samples. We are indebted to Dr. Thomas Hartmann (Martinsried, Germany) for performing the diffraction experiments. Diffraction of the Asp-85 → Glu bacteriorhodopsin sheets showed them to be highly ordered in both blue and red states of the chromophore.

Stationary spectra were measured with a Shimadzu UV-250 spectrophotometer outfitted with a cryostat for low temperature measurements as before [44], less otherwise stated, however, all spectra were determined at 22°C. Scattering curves constructed from hydroxylamine bleached samples were subtracted from the measured spectra. Time-resolved difference spectra were measured after subnanosecond laser excitation with a gated multichannel analyzer described earlier [45]. Non-linear regression analysis was with a program which utilized Marquardt-Levenberg algorithm. In some cases absorption changes at 410 nm were determined in a single wavelength instrument [41]. Action spectra for the photoproduction of the *M* intermediate were obtained with an excimer/dye laser.

Transport of protons in cell envelope vesicles was measured as before [20]. In order to reduce contributions from halorhodopsin and interference from the sodium/proton antiporter present in these membranes, the vesicles were heated at 55°C for 5 min before the measurements (and allowed to recover for 1 h), and the light-dependent pH changes were measured in 4 M KCl.

Results

pH dependency of the chromophore spectrum

Fig. 1A (solid lines) shows absorption spectra for Asp85 → Glu bacteriorhodopsin in 0.4 M NaCl at different pH values between 3 and 10.7. The pH-dependent shifts were fully reversible. Although not readily discerned in this graph, above pH 7 a single isosbestic point was observed which shifted somewhat at more

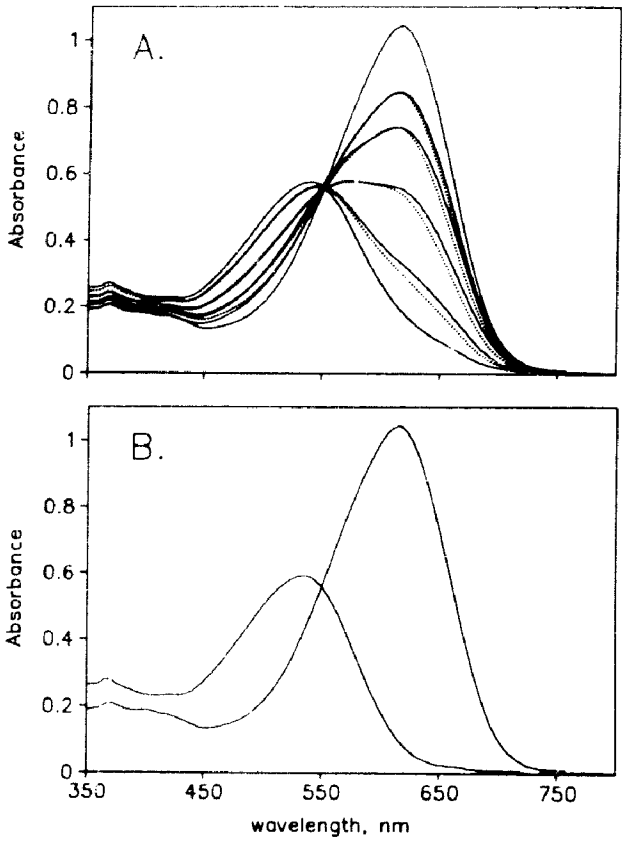

Fig. 1. Measured (A) and resolved (B) spectra of the blue and red species in Asp85 → Glu bacteriorhodopsin. (A) Solid lines: absorption spectra of dark-adapted samples at pH 4.0, 5.0, 7.0, 9.0, 10.0, and 10.7 (beginning with the spectrum of highest amplitude). Dotted lines: linear combinations of the two component spectra in (B) which best fitted the measured spectra. (B) Estimates of the spectra of the blue (maximum at 615 nm) and red (maximum at 532 nm) species in the mixtures shown in (A).

acidic pH. Nevertheless, as an approximation, we attempted to decompose the measured spectra into two component spectra derived from spectra near the pH extremes and shown in Fig. 1B. They have the characteristic skewed shape of rhodopsin spectra, and their maxima are at 532 nm ('red' species) and 615 nm ('blue' species). Combining these in proportions to best fit the measured spectra gave the dotted lines at intermediate pH values in Fig. 1A. The discrepancies on the red side of the spectra could be removed by using two slightly different spectra for blue species, and a single spectrum for the red species similar to that in Fig. 1B (not shown).

The calculated fraction of the red species in samples containing either no salt or 0.4 M NaCl, are shown in Fig. 2A and B, respectively, as functions of pH (○). Also shown are the amplitudes of the maximal absorption changes at 410 nm after flash excitation, due to the *M* intermediate (●), scaled (with the same factor in A and B) to coincide with the other data near pH 7. Description of the results required two widely separated pK_a values for the blue-red transition. This is different from an earlier study [36] with Asp85 → Glu bacteriorhodopsin expressed in *E. coli* and reincorporated into liposomes, where a single apparent pK_a near 6 was reported. The solid lines were calculated from a kinetic scheme in which 32% of the chromophore changed from blue to red with a pK_a of 5.4 and 68% changed from blue to red with a pK_a of 10.4 (Fig. 2A). In the presence of 0.4 M NaCl these pK_a values were 4.6 and 9.5, respectively (Fig. 2B).

The apparent heterogeneity of the sample with respect to the pK_a of the color transition probably explains the small discrepancy in the spectral fits when using two rather than three components (Fig. 1A). Rapid equilibrium between the two red species (or between the two blue species) would result in only one observable pK_a (as seen indeed with solubilized samples, cf. below). Thus, the simplest assumption is that the two blue species deprotonate independently to give two red species. When a sample was heated to 65°C for 30 min, cooled and its spectrum remeasured, a small but unambiguous shift from the red to the blue species was observed (not shown). This suggests that intercon-

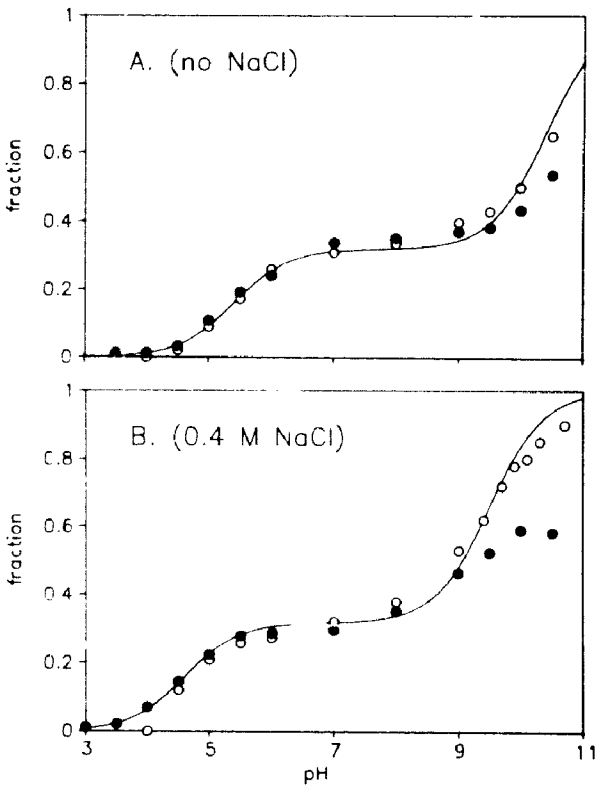

Fig. 2. pH dependency of the fractional concentration of the red species in Fig. 1 (○) and maximum amplitude at 410 nm after flash excitation (●). The latter data were scaled to roughly coincide with the concentrations at neutral pH. (A) Absence of added NaCl; (B) 0.4 M NaCl. The solid lines represent two independent red-blue chromophore equilibria, with pK_a values of 5.4 and 10.4 in the absence of NaCl, and 4.6 and 9.7 in its presence.

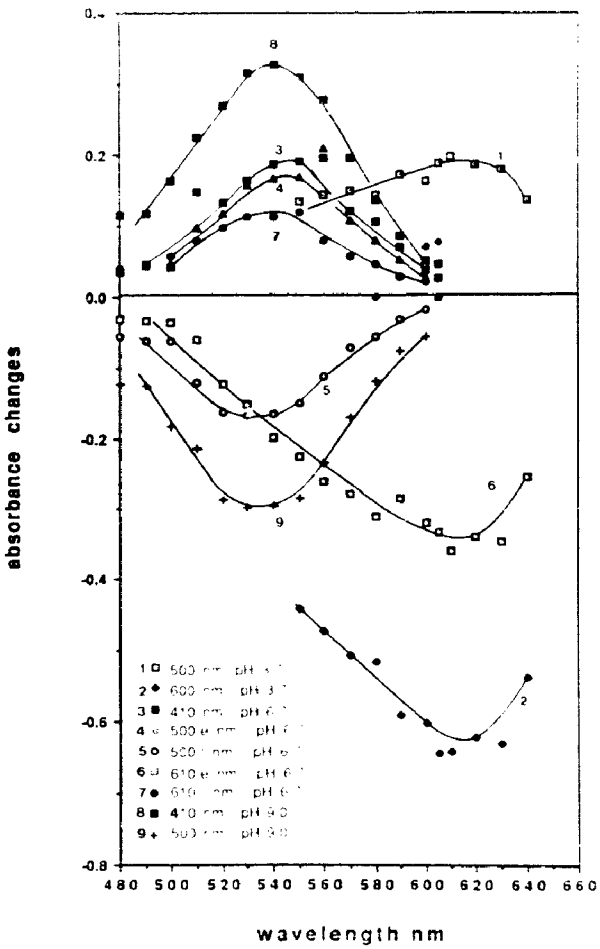

Fig. 3. Action spectrum for the photoproduction of the intermediates in the millisecond time range in the photocycles. Photoexcitation wavelength was varied by tuning a dye-laser, and maximal absorption changes at 410, 500 and 610 nm normalized to pulse intensity are shown at pH 3.7, 6.7 and 9.0. The selected wavelengths at the different times are indicative for the produced intermediates (positive amplitudes) or bleached initial states (negative amplitudes). Due to absorbance changes originating from the photocycle of the blue as well as the red form at two different times, the absorbance traces at 500 and 610 nm are labelled with 'e' (early) or 'l' (late) in the inset lower left. For details of lifetimes of the intermediates see Figs. 5, 7 and text.

version between the red species, and the consequent redistribution of the equilibria, is possible, but must proceed over a high activation barrier.

The amounts of M produced by flash excitation were consistent with the two pK_a values (Fig. 2A and B, ●), and argued that only the red species generated a deprotonated Schiff base. The increases in M yield, which corresponded to the second red species produced at high pH, were smaller than expected from the spectral transition, however. The action spectrum for the photoproduction of M (Fig. 3) confirmed that the intermediate originated from the red species in the mixtures. The decay kinetics for M were biphasic in these samples at all pH values (not shown). Thus, the two kinetic components did not correspond in any obvious way to the two postulated red species.

The pH dependency of the Asp85 → Glu chromophore changed dramatically after solubilization with Triton X-100. The spectra, in this case without added salt, are shown in Fig. 4A; they could be decomposed into blue and red species similar to those in Fig. 1B, but absorbing at 609 nm and 533 nm, respectively. The relative concentration of the red species in these samples showed monophasic change with pH (Fig. 4B). The chromophore was gradually and irreversibly lost below pH 4.5 and above pH 7.3, but this did not greatly change the results in Fig. 4. The line in Fig. 4B represents a double blue-red equilibrium, such as in Fig. 2A, but with rapid equilibration of the two red species. The apparent pK_a is 7.2; to fit the shallow pH dependency the dissociation of 0.5 protons was used in the equations. The latter was noticable also in the higher pK_a transitions in Fig. 2, and is undoubtedly

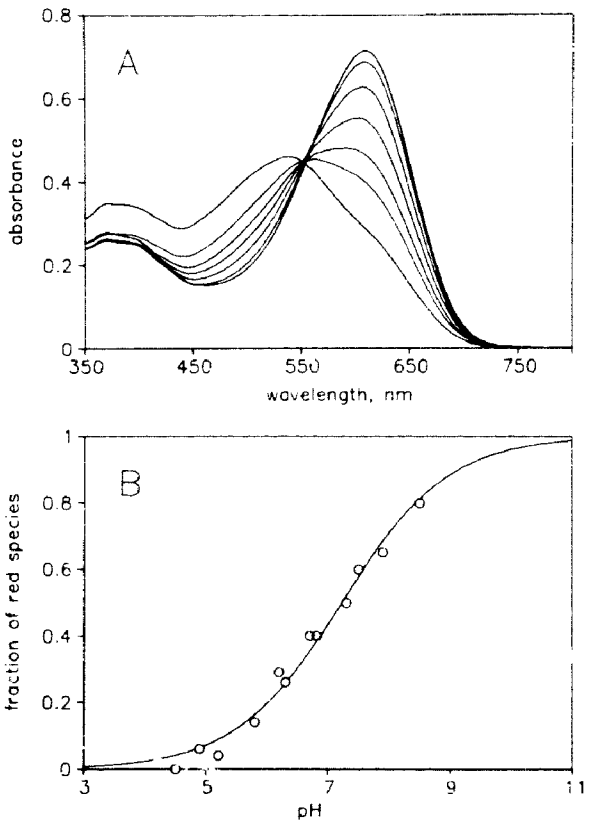

Fig. 4. Measured spectra of the blue and red species in Triton X-100 solubilized dark-adapted Asp85 → Glu bacteriorhodopsin, and their pH dependency. (A) Solid lines: absorption spectra of samples at pH 4.5, 5.1, 5.7, 6.2, and 6.7 (beginning with the spectrum of highest amplitude). (B) Fractional concentration of the red species, determined from decomposition of spectra, such as in (A), at various pH. The solid line represents an apparent pK_a of 7.2 for the transition, with $n = 0.5$ protons dissociating.

caused by surface effects, which are often seen in the pH dependency of bacteriorhodopsin properties [23].

Photochromism of the chromophore

As reported before for these samples [32] sustained (several min) illumination of dark-adapted Asp85 → Glu bacteriorhodopsin with white light did not produce shifts in its spectrum, characteristic of light-adaptation in the wild type. Sustained illumination with red light affected the spectra, however. It depleted 5–10% of both blue and red forms of the protein, and accumulated new species, with absorptions between 450 and 500 nm and between 350 and 400 nm, respectively (not shown). A first illumination with blue light had no detectable effect, but blue light fully reversed the shifts from previous illuminations with red light. Such photochromic behavior was reported for the blue form of wild-type bacteriorhodopsin [6,12,22], for halorhodopsin [43], and for the Arg82 → Gln mutant [34]. The photochromism of the samples did not affect our determinations of transient absorption changes (see below) because the measuring light contained enough blue component to prevent significant spectroscopic shifts.

Light-driven proton transport

Measurements of proton transport rates in cell envelope vesicles prepared from *H. halobium sp.* GRB strains 384 and wild-type (not shown) confirmed that (1) the action spectrum for transport placed the absorption maximum of the active Asp85 → Glu protein at about 530 nm, as determined earlier from photostationary currents [4] and proton uptake in reconstituted proteoliposomes [36], and (2) the transport activity of the Asp85 → Glu protein fell off more rapidly at low pH than that of the wild-type protein [36]. However, consistent with the behavior of the purified protein (Fig. 2), in our case decrease in the transport rate was seen only below pH 5.5, suggesting a pK_a well below this pH, while in the earlier study a much higher apparent pK_a was reported.

Photocycles of the blue and red species

The photoreaction of the blue forms of the Asp85 → Glu protein was determined at pH 4.0, in the presence of 0.4 M NaCl, using 610 nm excitation. Representative difference spectra at various delay times after the flash are shown in Fig. 5. Two interconversions were evident: (1) The initial intermediate, which absorbed on the red side of the spectrum of the parent protein was converted, in the μs time-range, to a blue-shifted species (Fig. 5A). (2) Decay of the latter, in the ms time-range, resulted in direct recovery of the parent chromophore (Fig. 5B). Estimates of the absorption spectra of these intermediates were obtained by resolving selected difference spectra into two components, as described elsewhere [39]. As shown in Fig.

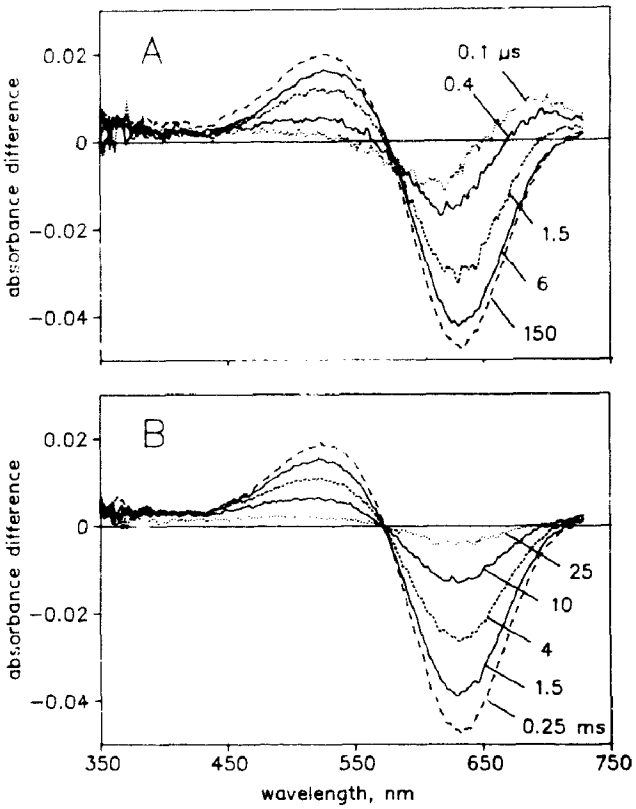

Fig. 5. Representative difference spectra of the blue species) at different delay times after 610 nm flash excitation, measured at pH 4.0, in the presence of 0.4 M NaCl. Absorption of the sample at 610 nm was about 0.8 (4 mm pathlength). (A) 100 ns to 150 μs time interval; (B) 250 μs to 25 ms time interval.

6A, the result of these calculations were spectra containing single peaks, with absorption maxima of 626 and 560 nm. Because of their resemblance to the K and L intermediates of the acid form of wild-type bacteriorhodopsin [14,38], they are labeled *K* and *L*. The measured difference spectra were then decomposed into algebraic sums of the component difference spectra calculated from the absolute spectra in Fig. 6A. The residuals of these fittings were within ±5% of the difference amplitudes. Thus, the component difference spectra accounted satisfactorily for the measured difference spectra. The weighting factors, which were the fractional concentrations of the intermediates [39] are shown versus the times after the flash in Fig. 6B. Up to 0.4 ms they added up to 1 at each time-point, indicating that no recovery of the parent chromophore had taken place. After this time, the disappearance of L was fully explained with the recovery of the blue species (cf. the isosbestic point in Fig. 5B).

In a similar way, the photoreaction of the red forms was determined at pH 10.5 in the presence of 0.4 M NaCl, with 520 nm excitation. Fig. 7 shows representative difference spectra at different delay times, which revealed three transitions: (1) production of M (peak

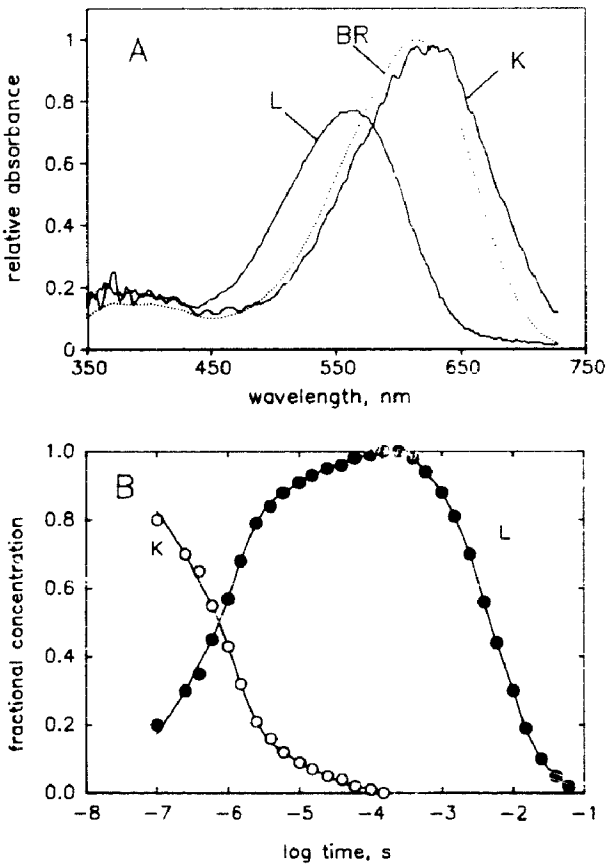

Fig. 6. Photoreaction of the blue species(s): calculated spectra for the intermediates labeled as K and L (A) and their kinetics (B), from data such as given in Fig. 4. The dotted line in (A) (labeled as BR) is the spectrum of the blue species(s), given for comparison.

near 410 nm) from the initial red-shifted intermediate on the μs time-scale (Fig. 7A), (2) decay of M, which generated a second red-shifted species on the ms time-scale (Fig. 7B), and (3) regeneration of the parent spectrum from the latter species without other detectable intermediates (not shown). Estimates for the absorption spectra of the three detected intermediates are given in Fig. 8A. The spectrum of the blue-shifted species identified it unambiguously as M. The other species are labeled as K and N, for reasons which will be given in the Discussion. The M of the Asp85 → Glu protein absorbed at 413 nm, the other two species at 570 nm and 585 nm, respectively. The kinetics of their rise and decay are shown in Fig. 8B. As with the blue species, the decomposition of the measured difference spectra into the three component difference spectra accounted for virtually all of the absorption changes.

We had attempted to describe the two photocycles from flash-induced difference spectra also at pH 7, where both blue and red species would contribute to the changes. Using 610 nm and 520 nm excitation wavelengths biased the results in favor of the photointermediates of the blue and red species, respectively, but even so, mixtures of species from both photocycles were obtained in all cases. Resolution of these, on the basis of the component spectra determined at higher and lower pH, proved to be not feasible because (a) the difference in the spectra of the two blue forms (with high and low pK_a, cf. Figs. 1 and 2) shifted the blue depletion peak somewhat at pH 7 from what was observed at pH 4, and (b) in the photocycle of the red forms at pH 7 two additional, greatly red-shifted intermediates appeared, one at the earliest delay times, and the other at the latest delay times (probably an O-like species). The kinetics of M could be evaluated unambiguously in spite of these complications because its absorption band near 410 nm is well separated from the others. Fig. 9A shows the amplitude of M as a function of delay time at pH 7.0 ( ), and the fit of two exponentials for the rise and two for the decay (line). The M amplitudes at pH 10.5, similarly fitted to four exponentials (from Fig. 8B) are also included (●). For comparison, M kinetics and exponential fits for wild-type bacteriorhodopsin at pH 7.0 and 10.5 are given in Fig. 9B (data from Fig. 4 in Ref. 42). The M kinetics for the Asp85 → Glu mutant (in Fig. 9A) could be thereby compared with those of wild-type bacteriorhodopsin (Fig. 9B): (a) At pH 7.0, but not at pH 10.5,

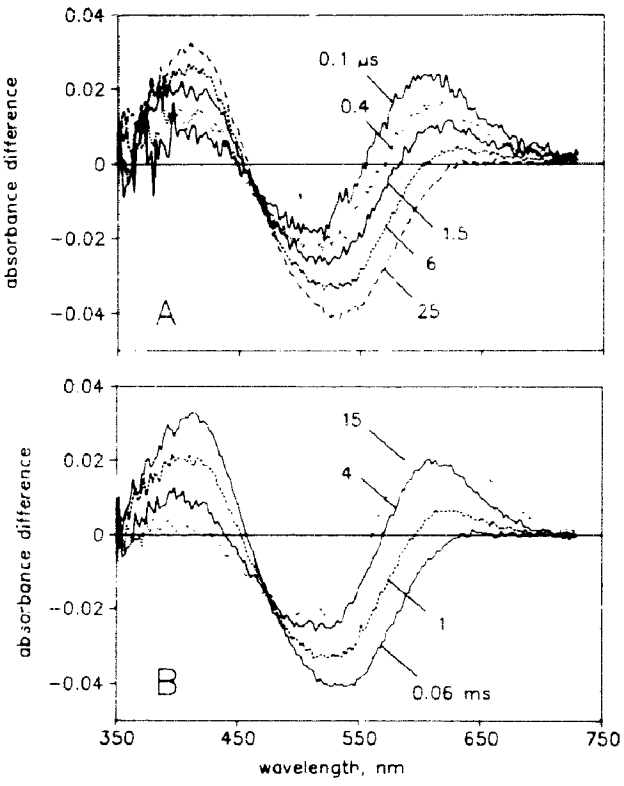

Fig. 7. Representative difference spectra of the red species(s) at different delay times after 520 nm flash excitation, measured at pH 10.5, in the presence of 0.4 M NaCl. Absorption of the sample at 532 nm was about 0.8 (4 mm pathlength). (A) 100 ns to 25 μs time interval; (B) 60 μs to 15 ms time interval.

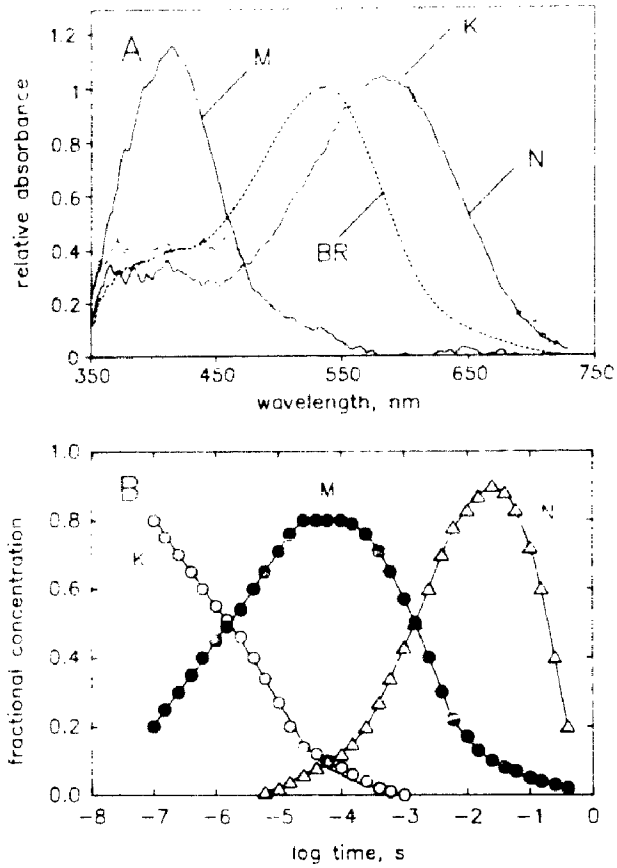

Fig. 8. Photoreaction of the red species' calculated spectra for the intermediates labeled as K, M, and N (A) and their kinetics (B), from data such as given in Fig. 6. The dotted line in (A) (labeled as BR) is the spectrum of the red species(s), given for comparison.

both components of the rise of M were dramatically faster in the Asp85 → Glu mutant than in wild-type. Thus, at pH 7 the two time constants in wild-type bacteriorhodopsin were 12 μs and 116 μs, with weights of 16% and 84%, while in the mutant these parameters were 1 μs (72%) and 15 μs (28%). The overall rise time was thus nearly two orders of magnitude greater in the mutant. (b) The decay of M in wild-type bacteriorhodopsin at pH 7 was described by a single exponential with a time constant of 3.5 ms, but at higher pH it assumed, increasingly, biphasic character. At pH 10.5 the two time constants in Fig. 9B were 1.1 ms and 76 ms, with weights of 80% and 20%. Importantly, the Asp85 → Glu protein showed similar behavior, although with a somewhat shifted pH dependency. Thus, in Fig. 9A at pH 7 the two decay components had time constants of 1.2 ms (44%) and 18 ms (56%), while at pH 10.5 they were 2.6 ms (81%) and 90 ms (19%).

Discussion

We found that replacement of Asp-85 with glutamate resulted not simply in the rise of a single pK_a for the purple-blue transition, as reported before [36]. Instead, two apparently separate not readily interconvertible conformations with widely different pK_a values were detected, and the spectrum of the two deprotonated forms exhibited a significant (36 nm) blue-shift relative to wild-type (Fig. 1 and 2). Since illumination of both deprotonated species produced M (Fig. 2), they must have both contained all-*trans* chromophores. An important difference between purple membrane sheets and *E. coli* expressed bacteriorhodopsin is the lack of crystalline structure in the latter, as shown by recently published spectra of induced CD [9]. The reasons for this are not clear. Converting the Asp85 → Glu protein from a two-dimensional crystalline array to monomers in detergent micelles resulted in the merging of the two pK_a values into one (Fig. 4). The reports on *E. coli* expressed bacteriorhodopsin are difficult to evaluate because the spectral titrations were shown as wavelength maxima of spectral mixtures vs. pH [36]. Although we found that this methods representation would have missed many of the details in our data, it

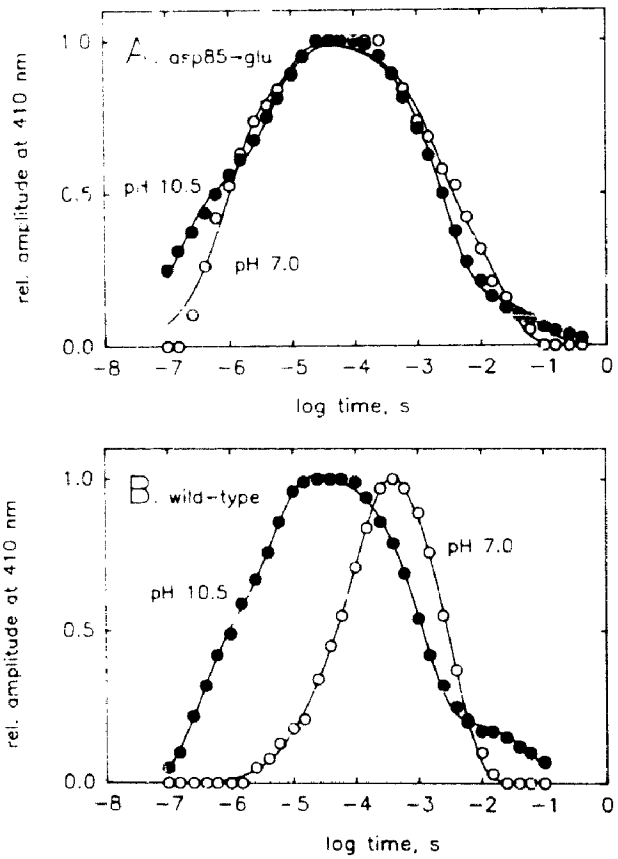

Fig. 9. Kinetics of M rise and decay. (A) Asp85 → Glu bacteriorhodopsin at pH 7.0 (○) and at pH 10.5 (●, data from Fig. 8B); (B) Wild-type bacteriorhodopsin at pH 7.0 (○) and 10.5 (●). The data in (B) are from Fig. 4 in Ref. 40. The relative amplitudes of the absorption changes at 410 nm are shown vs the delay time after photoexcitation (520 nm laser pulse for the mutant, 580 nm for wild-type). The lines represent non-linear regression fits, with two rise and one or two decay components as discussed in the text.

does appear that there are differences between the results, and they are mainly due to the presence or absence of crystalline sheets. It seems likely that the two Asp85 → Glu conformations identified by the two pK_a values exist also in the detergent micelles and proteoliposomes, but rapid equilibrium between them prevented the observation of separated pK_a values.

The photocycle of the Asp85 → Glu blue form(s) was quite similar to that of the blue form of wild-type bacteriorhodopsin [16,38], confirming earlier suggestions that the two kinds of blue chromophores are analogous. On photoexcitation the Asp85 → Glu blue forms produced the K- and L-like intermediates found in the photocycle of the wild-type blue protein, and no *M* (Fig. 6). Since the photoreaction sequence did not proceed as far as M, the intermediates could be identified unambiguously as K and L. Besides their pK_a values (Fig. 2), the two Asp85 → Glu blue forms differed only in a minor way in the chromophore spectra (not resolved in Fig. 1B); presumably the spectra of their photoproducts were also similar. The kinetics of the K → L transition (Fig. 6B) were not described by a single exponential; some or all of this complexity may have originated from differences in the K to L interconversions for the two blue forms. In wild-type bacteriorhodopsin, however, such deviations from exponential kinetics could be accounted for with back-reactions [39,40,42] and these are very likely present here also.

Since the absorption spectrum of the red forms was about 36 nm blue-shifted from that of wild-type bacteriorhodopsin, identification of the photoproducts could not be based simply on their absorption maxima. The species which followed M absorbed, for example, at 585 nm (Fig. 8A). This is 53 nm red-shifted from the band of the red species, and might be considered, superficially, the equivalent of O, a similarly red-shifted intermediate which appears after M in the wild-type protein. The kinetics argue for a different conclusion, however. At pH 10.5 the faster phase of the M decay corresponded to the rise of this intermediate, and the slower phase to its decay (Fig. 8B). It is N which has this kind of relationship to M in wild-type bacteriorhodopsin [27,40], interpreted as arising from the proton transfer and isomerization reactions, M ↔ N → O. The large accumulation of the intermediate at high pH also suggested that it must be the equivalent of N, since O is not observable at pH much above 7 in wild-type bacteriorhodopsin [21,41]. As expected from this, there was an indication of another, possibly *O* like intermediate in the Asp85 → Glu photocycle at pH 7 (cf. Results).

The precursor of M absorbed at 570 nm, i.e., 38 nm red-shifted from the absorption band of its parent, which is assigned as a K-like intermediate. In this case, the reason that L was not observed (Fig. 8B) would be that an unusually rapid L → M reaction had lowered its transient accumulation. Illumination at 80 K at pH 10.5 and warming to various temperatures up to 200 K (not shown) revealed also only one (red-shifted) intermediate before M.

The observed accelerated rise of M in the Asp85 → Glu protein at pH 7 (Fig. 9A), relative to wild-type (Fig. 9B), confirms earlier reports [4,28]. Interestingly, at higher pH the rise of M becomes much more rapid in wild-type bacteriorhodopsin (Fig. 9B; Ref. 40) and approaches that in the mutant. The origin of the biphasic rise was attributed to the L ↔ M equilibration reaction [39,40] in the wild-type protein, and this interpretation should apply for the mutant also. The decay of M contained two time-constants at both pH 7 and 10.5 (Figs. 8B and 9A); these were better separated at the higher pH. Biphasic M rise and decay in wild-type bacteriorhodopsin, observed mostly at pH > 7, has been long attributed to two M species in parallel photocycles [5,7,14,18], but recent models account for it satisfactorily with a single photocycle containing a significant N → M back-reaction and the slowing of the N decay at higher pH [1,27,39,40], which produce a pH dependent second, slower decay component. The similarity of the pH dependencies of the decay kinetics of M in the Asp85 → Glu and wild-type bacteriorhodopsin (Figs. 7B and 8) indicates good analogy between the two systems. Differences between the mutant and wild-type proteins were mainly in the decay of the intermediate labeled as K and in the rise of N, which contained additional time-constants, with small amplitudes, in the mutant (Fig. 8B). The origin of these may be the heterogeneity of the red species at high pH (Fig. 2).

A molecular explanation for the observed splitting of a single pK_a for the purple-blue transition in wild-type bacteriorhodopsin into two widely separated pK_a values in the Asp85 → Glu mutant is more problematical. These pK_a values are presumed to refer to the protonation of the residue at position 85, and will be influenced by neighboring groups. It seems likely that the cause of the two pK_a values is found in the dispositions of neighboring residues, either because disruptions of specific interactions or forming others (e.g., with Arg-82), or because of altered packing in this region of the protein residues. The lower of the pK_a values observed (4.6–5.4, depending on ionic strength) is normal for a carboxyl group exposed to the medium. The higher pK_a (9.7–10.4, depending on the ionic strength) indicates a highly unusual environment which stabilizes the protonated carboxyl group by as much as 6.7 kcal/mol. Thus, when the length of residue 85 was increased by a methylenic group, the Schiff base seemed to sample different charge environments before and during the photocycle than it does in wild-type bacteriorhodopsin.

Acknowledgements

Funded in part by grants to L.K.L. from the National Aeronautics and Space Administration (NAGW-212) and the National Institutes of Health (GM 29498).

References

1 Ames, J.B., Fodor, S.P.A. and Mathies, R.A. (1990) Biochemistry 15, 5631–5640.
2 Aton, B., Doukas, A.G., Callender, R.H., Becher, B. and Ebrey, T.G. (1977) Biochemistry 16, 2995–2999.
3 Braiman, M.S., Mogi, T., Marti, T., Stern, L.J., Khorana, H.G. and Rothschild, K.J. (1988) Biochemistry 27, 8516–8520.
4 Butt, H.-L., Fendler, K., Bamberg, E., Tittor, J. and Oesterhelt, D. (1989a) EMBO J. 8, 1657–1663.
5 Butt, H.-J., Fendler, K., Dér, A. and Bamberg, E. (1989b) Biophys. J. 56, 851–859.
6 Chang, C.H., Liu, S., Jonas, R. and Govindjee, R. (1987) Biophys. J. 51, 137a.
7 Dancsházy, Zs., Govindjee, R. and Ebrey, T.G. (1988) Proc. Natl. Acad. Sci. USA 85, 6358–6361.
8 Dencher, N.A. and Heyn, M.P. (1978) FEBS. Lett. 96, 322–326.
9 Du-Jeon-Jang, El-Sayed, M.A., Stern, L.J., Mogi, T. and Khorana, H.G. (1990) FEBS Lett. 262, 155–158.
10 Edgerton, M.E., Moore, T.A. and Greenwood, C. (1980) Biochem. J. 189, 413–420.
11 Fischer, U. and Oesterhelt, D. (1979) Biophys. J. 28, 211–230.
12 Fischer, U., Towner, P. and Oesterhelt, D. (1981) Photochem. Photobiol. 33, 529–537.
13 Gerwert, K., Hess, B., Soppa, J. and Oesterhelt, D. (1989) Proc. Natl. Acad. Sci. USA 86, 4943–4947.
14 Hanamoto, J.H., Dupuis, P. and El-Sayed, M.A. (1984) Proc. Natl. Acad. Sci. USA 81, 7083–7087.
15 Holz, M., Drachev, L.A., Mogi, T., Otto, H., Kaulen, A.D., Heyn, M.P., Skulachev, V.P. and Khorana, H.G. (1989) Proc. Natl. Acad. Sci. USA 86, 2167–2171.
16 Kobayashi, T., Ohtani, H., Iwai, J.-I., Ikegami, A. and Uchiki, H. (1983) FEBS Lett. 162, 197–200.
17 Koch, M., Dencher, N., Oesterhelt, D., Plöhn, H., Rapp, G. and Büldt, G. (1991) EMBO J. 10, 521–526.
18 Kouyama, T., Nasuda-Kouyama, A., Ikegami, A., Mathew, M.K. and Stoeckenius, W. (1988) Biochemistry 27, 5855–5863.
19 Lanyi, J.K. and MacDonald, R.E. (1979) Methods Enzymol. 55, 777–780.
20 Lanyi, J.K. and Oesterhelt, D. (1982) J. Biol. Chem. 257, 2674–2677.
21 Lu, Q., Govindjee, R. and Ebrey, T.G. (1984) Proc. Natl. Acad. Sci. USA 81, 7079–7082.
22 Maeda, A., Iwasa, T. and Yoshizawa, T. (1980) Biochemistry 19, 3825–3831.
23 Miller, A. and Oesterhelt, D. (1990) Biochim. Biophys. Acta 1020, 57–64.
24 Mogi, T., Stern, L.J., Marti, T., Chao, B.H. and Khorana, H.G. (1988) Proc. Natl. Acad. Sci. USA 85, 4148–4152.
25 Mowery, P.C., Lozier, R.H., Chae, Q., Tseng, Y.W., Taylor, M. and Stoeckenius, W. (1979) Biochemistry 18, 4100–4107.
26 Oesterhelt, D. and Stoeckenius, W. (1974) Methods Enzymol. 31, 667–678.
27 Otto, H., Marti, T., Holz, M., Mogi, T., Lindau, M., Khorana, H.G. and Heyn, M.P. (1989) Proc. Natl. Acad. Sci. USA 86, 9228–9232.
28 Otto, H., Marti, T., Holz, M., Mogi, T., Stern, L.J., Engel, F., Khorana, H.G. and Heyn, M.P. (1990) Proc. Natl. Acad. Sci. USA 87, 1018–1022.
29 Pettei, M.J., Yudd, A.P., Nakanishi, K., Henselman, R. and Stoeckenius, W. (1977) Biochemistry 16, 1955–1959.
30 Rothschild, K.J., Zagaeski, M. and Cantore, W.A. (1981) Biochem. Biophys. Res. Commun. 103, 483–489.
31 Soppa, J. and Oesterhelt, D. (1989) J. Biol. Chem. 264, 13043–13048.
32 Soppa, J., Otomo, J., Straub, J., Tittor, J., Meessen, S. and Oesterhelt, D. (1989) J. Biol. Chem. 264, 13049–13056.
33 Stern, L.J., Ahl, P.L., Marti, T., Mogi, T., Duñach, M., Berowitz, S., Rothschild, K. and Khorana, G. (1989) Biochemistry 28, 10035–10042.
34 Stern, L.J. and Khorana, H.G. (1989) J. Biol. Chem. 264, 14202–14208.
35 Stoeckenius, W., Lozier, R.H. and Bogomolni, R.A. (1979) Biochim. Biophys. Acta 505, 215–278.
36 Subramaniam, S., Marti, T. and Khorana, H.G. (1990) Proc. Natl. Acad. Sci. USA 87, 1013–1017.
37 Tittor, J., Soell, C., Oesterhelt, D., Butt, H.-J. and Bamberg, E. (1989) EMBO J. 8, 3477–3482.
38 Váró, G. and Lanyi, J.K. (1989) Biophys. J. 56, 1143–1151.
39 Váró, G. and Lanyi, J.K. (1990) Biophys. J. 59, 313–322.
40 Váró, G. and Lanyi, J.K. (1990) Biochemistry 29, 2241–2250.
41 Váró, G. and Lanyi, J.K. (1990) Biochemistry 29, 6858–6865.
42 Váró, G. and Lanyi, J.K. (1991) Biochemistry 30, 5016–5022.
43 Zimányi, L. and Lanyi, J.K. (1987) Biophys. J. 52, 1007–1013.
44 Zimányi, L., Ormos, P. and Lanyi, J.K. (1989) Biochemistry 28, 1656–1661.
45 Zimányi, L., Keszthelyi, L. and Lanyi, J.K. (1989) Biochemistry 28, 5165–5172.